Coupled Systems Mechanics, *Vol. 9, No. 6 (2020) 575-597*
DOI: https://doi.org/10.12989/csm.2020.9.6.575

Effect of porosity distribution rate for bending analysis of imperfect FGM plates resting on Winkler-Pasternak foundations under various boundary conditions

Kablia Aicha[1,3], Benferhat Rabia[1,2], Tahar Hassaine Daouadji*[1,2] and Ahmed Bouzidene[3]

[1]Laboratory of Geomatics and Sustainable Development, University of Tiaret, Algeria
[2]Department of Civil Engineering, University of Tiaret, Algeria
[3]Department of Mechanical Engineering, University of Tiaret, Algeria

(Received July 29, 2020, Revised December 2, 2020, Accepted December 3, 2020)

Abstract. Equilibrium equations of a porous FG plate resting on Winkler-Pasternak foundations with various boundary conditions are derived using a new refined shear deformation theory. Different types of porosity distribution rate are considered. Governing equations are obtained including the plate-foundation interaction. This new model meets the nullity of the transverse shear stress at the upper and lower surfaces of the plate. The novel rule of mixture is proposed to describe and approximate material properties of the FG plates with different distribution case of porosity. The validity of this theory is studied by comparing some of the present results with other higher-order theories reported in the literature. Effects of variation of porosity distribution rate, boundary conditions, foundation parameter, power law index, plate aspect ratio, side-to-thickness ratio on the deflections and stresses are all discussed.

Keywords: functionally graded materials; refined plate theory; various boundary conditions; imperfect plates; effect of porosity distribution rate

1. Introduction

In recent years, the concept of functionally graded materials (FGMs) was first introduced by material scientists in the Sendai area of Japan. Functionally graded materials (FGMs) are a class of composites that have continuous variation of material properties from one surface to another and thus eliminate the stress concentration found in laminated composites. The FGMs which are often isotropic and nonhomogeneous, are made from a mixture of two materials to achieve a composition that provides a certain functionality. In FGM, these problems are avoided or reduced by gradual variation of the constituents' volume fraction rather than abruptly changing it across the interface. Power-law function and exponential function are commonly used to describe the variations of material properties of FGM. However, in both power-law and exponential functions, the stress concentrations appear in one of the interfaces in which the material is continuously but rapidly changing.

*Corresponding author, Professor, E-mail: daouadjitahar@gmail.com

http://www.techno-press.org/?journal=csm&subpage=8 ISSN: 2234-2184 (Print), 2234-2192 (Online)

Since the shear deformation effects are more pronounced in thick functionally graded materials (FGM) plates, shear deformation theories should be used to analyze FGM plates. In addition, the increasing use of plates as structural components in various fields such as marine technology; civil and aerospace has made it necessary to study their mechanical behavior. Several studies have been undertaken on the mechanical behavior of FGM plates. All authors (Abdelaziz *et al*. 2017, Adim 2018, Abualnour *et al*. 2018, Ait Atmane *et al*. 2015, Carrera *et al*. 2011, Chikr *et al*. 2020, Refrafi *et al*. 2020, Bousahla *et al*. 2020, Bellal *et al*. 2020, Bensattalah *et al*. 2018, Daouadji *et al*. 2016b, Hamrat *et al*. 2020, Hassaine Daouadji 2013, Hassaine Daouadji *et al*. 2020, Tounsi *et al*. 2020, Shariati *et al*. 2020, Al-Furjan *et al*. 2020, Al-Furjan *et al*. 2020, Benhenni *et al*. 2019, Benferhat *et al*. 2018, Bensattalah *et al*. 2020, Boukhlif *et al*. 2019, Boulefrakh *et al*. 2019, Chaabane *et al*. 2019, Benferhat *et al*. 2016b, El-Haina *et al*. 2017, Hassaine Daouadji *et al* 2016, Demirhan *et al*.2019, Khalifa *et al*.2018, Reddy 2001, Slimane *et al*. 2018, Zenkour 2009), have studied the bending of a simply supported polygonal plate with a property gradient given by a order shear deformation theory. The first-order shear deformation theory (FSDT) gives acceptable results, but requires a shear correction factor. Whereas, the higher-order shear deformation theories (HSDTs) do not require a shear correction factor, but their equations of motion are more complicated than those of the FSDT. Therefore, Tounsi (2013) has developed a four variable plate theory. The four variable plate theory of Tounsi (2013) accounts for a parabolic variation of the transverse shear strains through the thickness, and hence, a shear correction factor is not required. The displacement field of the four variable plate theory is chosen based on the partition of the transverse displacements into the bending and shear parts. The most interesting feature of the four variable plate theory is that it contains fewer unknowns and governing equations than those of the FSDT and does not require a shear correction factor. Thus, it is the most efficient theory. The four variable plate theory was first developed for isotropic plates, and recently extended to FGM plates, FGM sandwich plates, and nanoplates.

In general, higher order shear and normal deformation theories which consider thickness stretching effect can be implemented using the unified formulation initially proposed by several authors (Ait Yahia *et al*.2015, Hassaine Daouadji *et al*. 2019, Mohamed Amine *et al*. 2019, Rabahi *et al*. 2019, Rabia *et al*. 2016, Benchohra *et al*. 2018, Kaddari *et al*. 2020, Addou *et al*. 2019, Medani *et al*. 2019, Bourada *et al*. 2019, Abdederak *et al*. 2018, Abdelhak *et al*. 2016, Benferhat *et al*. 2019, Belkacem *et al*. 2016, Benhenni *et al*. 2018, Rabhi *et al*. 2020, Benferhat *et al*. 2016a, Belabed *et al*. 2018, Cooke *et al*. 1983, Bensattalah T *et al*. 2016, Bouakaz *et al*. 2014, Bekki *et al*. 2019, Chaded *et al*. 2018, Chergui *et al*. 2019, Daouadji *et al*. 2016a, Tounsi *et al*.2013, Bourada *et al*. 2020, Matouk *et al*. 2020, bane *et al*. 2019, Menasria *et al*. 2020, Rahmani *et al*. 2020, Balubaid *et al*. 2019, Rabahi *et al*. 2020, Tounsi *et al*. 2008, Tahar *et al*. 2016, Alimirzaei *et al*. 2019, Sahla *et al*. 2019, Karami *et al*. 2019, Zine *et al*. 2020, Wattanasakulponga 2014, Lee *et al*.2002, Mokhtar *et al*. 2018, Thai *et al*. 2013, Younsi *et al*. 2018, Yazid *et al*. 2018, Zaoui *et al*. 2019). Many higher order shear and normal deformation theories have been proposed in the literature. These theories are cumbersome and computationally expensive since they invariably generate a host of unknowns. Although some well-known quasi-3D theories developed by Zenkour (2018) and recently by Mantari (2012) have six unknowns, they are still more complicated than the FSDT. Thus, there is a scope to develop an accurate higher order shear and normal deformation theory, which is relatively simple to use and simultaneously retains important physical characteristics. Indeed, Tounsi (2013) presented recently a quasi-3D sinusoidal shear deformation theory, with only five unknowns for bending and free vibration analysis of FGM plates.

In this paper, a new and refined theory for the flexural analysis of imperfect FGM plates under different boundary conditions taking into account the porosities that can possibly occur inside

Table 1 Summary table which groups the different distribution of porosity in the FGM (Ceramic / Metal)

Types	Distribution of porosity rate in the FGM		Young module
	Ceramic	*Metal*	
Type-I	Without porosity		$E(z) = (E_c - E_m)(\frac{z}{h} + \frac{1}{2})^k + E_m$ (14a)
Type-II	50%	50%	$E(z) = (E_c - E_m)(\frac{z}{h} + \frac{1}{2})^k + E_m - (E_c + E_m)\frac{\alpha}{2}$ (14b)
Type-III	60%	40%	$E(z) = (E_c - E_m)(\frac{z}{h} + \frac{1}{2})^k + E_m - (3E_c + 2E_m)\frac{\alpha}{5}$ (14c)
Type-IV	40%	60%	$E(z) = (E_c - E_m)(\frac{z}{h} + \frac{1}{2})^k + E_m - (2E_c + 3E_m)\frac{\alpha}{5}$ (14d)
Type-V	75%	25%	$E(z) = (E_c - E_m)(\frac{z}{h} + \frac{1}{2})^k + E_m - (3E_c + E_m)\frac{\alpha}{4}$ (14e)
Type-VI	25%	75%	$E(z) = (E_c - E_m)(\frac{z}{h} + \frac{1}{2})^k + E_m - (E_c + 3E_m)\frac{\alpha}{4}$ (14f)

functional gradation materials (FGM) during their manufacture. Numerical examples are presented to illustrate the precision and the efficiency of the present solution, by showing the influence of the distribution rate of the porosity of the base material on the mechanical behavior of the FGM plate.

2. Problem formulation

2.1 Constitutive relations of (metal/ ceramic) functionally graded plates

Consider an imperfect FGM with a porosity volume fraction, α (α << 1), distributed evenly among the metal and ceramic, the modified rule of mixture proposed by Wattanasakulpong and Ungbhakorn (2014) is used as (Benferhat *et al*. 2016a, Hassaine Daouadji 2017, Rabahi *et al*. 2016)

$$P = P_m(V_m - \frac{\alpha}{2}) + P_c(V_c - \frac{\alpha}{2}) \tag{1}$$

Now, the total volume fraction of the metal and ceramic is: $V_m + V_c = 1$ and the power law of volume fraction of the ceramic is described as (Table 1):

$$V_c = (\frac{z}{h} + \frac{1}{2})^k \tag{2}$$

Hence, all properties of the imperfect FGM can be written as (Benferhat *et al*. 2016a)

$$\rho(z) = (\rho_c - \rho_m)(\frac{z}{h} + \frac{1}{2})^k + \rho_m - (\rho_c + \rho_m)\frac{\alpha}{2} \tag{3}$$

It is noted that the positive real number k ($0 \leq k < \infty$) is the power law or volume fraction index, and z is the distance from the mid-plane of the FG plate. The FG plate becomes a fully ceramic plate when k is set to zero and fully metal for large value of k.

Thus, the Young's modulus (E) and material density (ρ) equations of the imperfect FGM plate can be expressed as (Benferhat *et al*. 2016a), including a summary table which groups together the different porosity distributions in the FGMs will be presented in Table 1.

$$E(z) = (E_c - E_m)(\frac{z}{h} + \frac{1}{2})^k + E_m - (E_c + E_m)\frac{\alpha}{2} \tag{4}$$

$$\rho(z) = (\rho_c - \rho_m)(\frac{z}{h} + \frac{1}{2})^k + \rho_m - (\rho_c + \rho_m)\frac{\alpha}{2} \tag{5}$$

However, Poisson's ratio (ν) is assumed to be constant. The material properties of a perfect FG plate can be obtained when α is set to zero.

As

$$\boldsymbol{V_c + V_m = 1 \Rightarrow V_c = 1 - V_m} \tag{6}$$

and

$$\boldsymbol{V_c = (\frac{z}{h} + \frac{1}{2})^k} \tag{7}$$

Type I: *perfect FG plate (Without porosity* $\alpha = 0$*)*

$$E(z) = (E_c - E_m)(\frac{z}{h} + \frac{1}{2})^k + E_m \tag{8}$$

Type II: *50% Ceramic, 50% Metal*

$$\boldsymbol{E = E_m(V_m - \frac{\alpha}{2}) + E_c(V_c - \frac{\alpha}{2})} \tag{9a}$$

$$E(z) = (E_c - E_m)(\frac{z}{h} + \frac{1}{2})^k + E_m - (E_c + E_m)\frac{\alpha}{2} \tag{9b}$$

Type III: *60% Ceramic, 40% Metal*

$$\boldsymbol{E = E_m(V_m - \frac{2\alpha}{5}) + E_c(V_c - \frac{3\alpha}{5})} \tag{10a}$$

$$E(z) = (E_c - E_m)(\frac{z}{h} + \frac{1}{2})^k + E_m - (3E_c - 2E_m)\frac{\alpha}{5} \tag{10b}$$

Type IV: *40% Ceramic, 60% Metal*

$$\boldsymbol{E = E_m(V_m - \frac{3\alpha}{5}) + E_c(V_c - \frac{2\alpha}{5})} \tag{11a}$$

$$E(z) = (E_c - E_m)(\frac{z}{h} + \frac{1}{2})^k + E_m - (2E_c - 3E_m)\frac{\alpha}{5} \tag{11b}$$

Type V: *75% Ceramic, 25% Metal*

$$\boldsymbol{E = E_m(V_m - \frac{\alpha}{4}) + E_c(V_c - \frac{3\alpha}{4})} \tag{12a}$$

$$E(z) = (E_c - E_m)(\frac{z}{h} + \frac{1}{2})^k + E_m - (3E_c - E_m)\frac{\alpha}{4} \tag{12b}$$

Type VI: *25% Ceramic, 75% Metal*

$$\boldsymbol{E = E_m(V_m - \frac{3\alpha}{4}) + E_c(V_c - \frac{\alpha}{4})} \tag{13a}$$

$$E(z) = (E_c - E_m)(\frac{z}{h} + \frac{1}{2})^k + E_m - (E_c - 3E_m)\frac{\alpha}{4} \tag{13b}$$

2.2 Theoretical formulations

2.2.1 Basic assumptions

Consider a plate of total thickness h and composed of functionally graded material through the thickness (Fig. 1). It is assumed that the material is isotropic and grading is assumed to be only

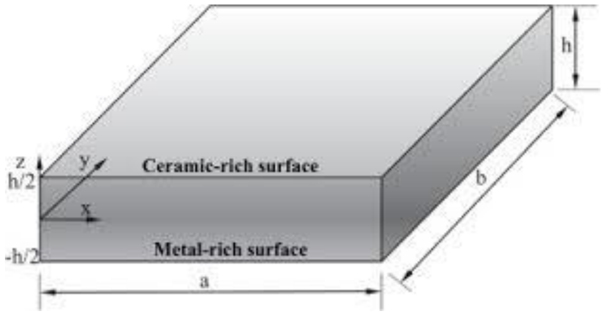

Fig. 1 Geometry of rectangular plate composed of FGM

through the thickness. The *xy* plane is taken to be the undeformed mid plane of the plate with the *z* axis positive upward from the mid plane.

- The displacements are small in comparison with the plate thickness and, therefore, strains involved are infinitesimal.
- The transverse displacement *w* includes three components of bending w_b and shear w_s. These components are functions of coordinates *x*, *y*, and time *t* only.

$$w(x,y,z,t) = w_b(x,y,t) + w_s(x,y,t) \tag{15}$$

- The transverse normal stress σ_z is negligible in comparison with in-plane stresses σ_x and σ_y.
- The displacements *U* in *x*-direction and *V* in *y*-direction consist of extension, bending, and shear components

$$U = u + u_b + u_s,\ V = v + v_b + v_s \tag{16}$$

- The bending components u_b and v_b are assumed to be similar to the displacements given by the classical plate theory. Therefore, the expression for u_b and v_b can be given as

$$u_b = -z\frac{\partial w_b}{\partial x},\ v_b = -z\frac{\partial w_b}{\partial y} \tag{17}$$

- The shear components u_s and v_s give rise, in conjunction with w_s, to the parabolic variations of shear strains γ_{xz}, γ_{yz} and hence to shear stresses σ_{xz}, σ_{yz} through the thickness of the plate in such a way that shear stresses σ_{xz}, σ_{yz} are zero at the top and bottom faces of the plate. Consequently, the expression for u_s and v_s can be given as

$$u_s = f(z)\frac{\partial w_s}{\partial x},\ v_s = f(z)\frac{\partial w_s}{\partial y} \tag{18}$$

2.2.2 Kinematics:

Based on the assumptions made in the preceding section, the displacement field can be obtained using Eqs. (15)-(18)

$$u(x,y,z) = u_0(x,y) - z\frac{\partial w_b}{\partial x} - z\left[1 - \sec h\left(\frac{\pi z^2}{h^2}\right) + \sec h\left(\frac{\pi}{4}\right)\left(1 - \frac{\pi}{2}\tanh\left(\frac{\pi}{4}\right)\right)\right]\frac{\partial w_s}{\partial x}$$
$$v(x,y,z) = v_0(x,y) - z\frac{\partial w_b}{\partial y} - z\left[1 - \sec h\left(\frac{\pi z^2}{h^2}\right) + \sec h\left(\frac{\pi}{4}\right)\left(1 - \frac{\pi}{2}\tanh\left(\frac{\pi}{4}\right)\right)\right]\frac{\partial w_s}{\partial y}$$
$$w(x,y,z) = w_b(x,y) + w_s(x,y) \tag{19}$$

where u_0 and v_0 are the mid-plane displacements of the plate in the x and y direction, respectively; w_b and w_s are the bending and shear components of transverse displacement, respectively, while $f(z)$ represents the functions of form; it is indeed a new theory of hyperbolic shear strain (Hassaine Daouadji 2016), determining the distribution of transverse shear strains and stresses along the thickness and is given by

$$f(z) = z[1 - sec\,h\,(\frac{\pi z^2}{h^2}) + sec\,h\,(\frac{\pi}{4})(1 - \frac{\pi}{2} tanh(\frac{\pi}{4})] \tag{20}$$

It should be noted that unlike the first-order shear deformation theory, this theory does not require shear correction factors. The kinematic relations can be obtained as follows

$$\varepsilon_x = \varepsilon_x^0 + z\,k_x^b + z[1 - sec\,h\,(\frac{\pi z^2}{h^2}) + sec\,h\,(\frac{\pi}{4})(1 - \frac{\pi}{2} tanh(\frac{\pi}{4})]\,k_x^s$$

$$\varepsilon_y = \varepsilon_y^0 + z\,k_y^b + z[1 - sec\,h\,(\frac{\pi z^2}{h^2}) + sec\,h\,(\frac{\pi}{4})(1 - \frac{\pi}{2} tanh(\frac{\pi}{4})]\,k_y^s$$

$$\gamma_{xy} = \gamma_{xy}^0 + z\,k_{xy}^b + z[1 - sec\,h\,(\frac{\pi z^2}{h^2}) + sec\,h\,(\frac{\pi}{4})(1 - \frac{\pi}{2} tanh(\frac{\pi}{4})]\,k_{xy}^s$$

$$\gamma_{yz} = 1 - \frac{d[z[1 - sec\,h(\frac{\pi z^2}{h^2}) + sec\,h(\frac{\pi}{4})(1 - \frac{\pi}{2} tanh(\frac{\pi}{4})]]}{dz}\,\gamma_{yz}^s$$

$$\gamma_{xz} = 1 - \frac{d[z[1 - sec\,h(\frac{\pi z^2}{h^2}) + sec\,h(\frac{\pi}{4})(1 - \frac{\pi}{2} tanh(\frac{\pi}{4})]]}{dz}\,\gamma_{xz}^s$$

$$\varepsilon_z = 0 \tag{20}$$

where

$$\varepsilon_x^0 = \frac{\partial u_0}{\partial x},\ k_x^b = -\frac{\partial^2 w_b}{\partial x^2},\ k_x^s = -\frac{\partial^2 w_s}{\partial x^2}$$

$$\varepsilon_y^0 = \frac{\partial v_0}{\partial y},\ k_y^b = -\frac{\partial^2 w_b}{\partial y^2},\ k_y^s = -\frac{\partial^2 w_s}{\partial y^2}$$

$$\gamma_{xy}^0 = \frac{\partial u_0}{\partial y} + \frac{\partial v_0}{\partial x},\ k_{xy}^b = -2\frac{\partial^2 w_b}{\partial x \partial y},$$

$$k_{xy}^s = -2\frac{\partial^2 w_s}{\partial x \partial y}\ \gamma_{yz}^s = \frac{\partial w_s}{\partial y},\ \gamma_{xz}^s = \frac{\partial w_s}{\partial x},$$

$$f'(z) = \frac{df(z)}{dz} = \frac{d[z[1 - sec\,h(\frac{\pi z^2}{h^2}) + sec\,h(\frac{\pi}{4})(1 - \frac{\pi}{2} tanh(\frac{\pi}{4})]]}{dz}$$

$$g(z) = 1 - f'(z) = 1 - \frac{d[z[1 - sec\,h(\frac{\pi z^2}{h^2}) + sec\,h(\frac{\pi}{4})(1 - \frac{\pi}{2} tanh(\frac{\pi}{4})]]}{dz} \tag{21}$$

The stress state in each layer is given by Hooke's law

$$\begin{Bmatrix} \sigma_x \\ \sigma_y \\ \tau_{yz} \\ \tau_{xz} \\ \tau_{xy} \end{Bmatrix} = \begin{bmatrix} \frac{E(z)}{1-\nu^2} & \frac{\nu E(z)}{1-\nu^2} & 0 & 0 & 0 \\ \frac{\nu E(z)}{1-\nu^2} & \frac{E(z)}{1-\nu^2} & 0 & 0 & 0 \\ 0 & 0 & \frac{E(z)}{2(1+\nu)} & 0 & 0 \\ 0 & 0 & 0 & \frac{E(z)}{2(1+\nu)} & 0 \\ 0 & 0 & 0 & 0 & \frac{E(z)}{2(1+\nu)} \end{bmatrix} \begin{Bmatrix} \varepsilon_x \\ \varepsilon_y \\ \gamma_{yz} \\ \gamma_{xz} \\ \gamma_{xy} \end{Bmatrix} \tag{23}$$

2.2.3 Governing equations

The governing equations of equilibrium can be derived by using the principle of virtual displacements. The principle of virtual work in the present case yields

$$\int_{-h/2}^{h/2}\int_{\Omega}\left[\sigma_x\delta\,\varepsilon_x+\sigma_y\delta\,\varepsilon_y+\tau_{xy}\delta\,\gamma_{xy}+\tau_{yz}\delta\,\gamma_{yz}+\tau_{xz}\delta\,\gamma_{xz}\right]d\Omega\,dz-\int_{\Omega}q\,\delta\,wd\Omega=0 \qquad (24)$$

where Ω is the top surface and q is the applied transverse load.

Substituting Eqs. (19) and (22) into Eq. (24) and integrating through the thickness of the plate, Eq (24) can be rewritten as

$$\begin{aligned}\int_{\Omega}\big[&N_x\delta\,\varepsilon_x^0+N_y\delta\,\varepsilon_y^0+N_{xy}\delta\,\varepsilon_{xy}^0+M_x^b\delta\,k_x^b+M_y^b\delta\,k_y^b+M_{xy}^b\delta\,k_{xy}^b+M_x^s\delta\,k_x^s\\&+M_y^s\delta\,k_y^s+M_{xy}^s\delta\,k_{xy}^s+S_{yz}^s\delta\,\gamma_{yz}^s+S_{xz}^s\delta\,\gamma_{xz}^s\big]d\Omega-\int_{\Omega}q\,\delta\,wd\Omega=0\end{aligned} \qquad (25)$$

where

$$\begin{Bmatrix}N_x, & N_y, & N_{xy}\\ M_x^b, & M_y^b, & M_{xy}^b\\ M_x^s, & M_y^s, & M_{xy}^s\end{Bmatrix}=\int_{-h/2}^{h/2}(\sigma_x,\sigma_y,\tau_{xy})\begin{Bmatrix}1\\ z\\ z[1-sec\,h(\frac{\pi z^2}{\frac{2}{h}})+sec\,h(\frac{\pi}{4})(1-\frac{\pi}{2}tanh(\frac{\pi}{4})]\end{Bmatrix}dz, \qquad (26)$$

$$\left(S_{xz}^s,S_{yz}^s\right)=\int_{-h/2}^{h/2}(\tau_{xz},\tau_{yz})(1-\frac{d[z[1-sec\,h(\frac{\pi z^2}{\frac{2}{h}})+sec\,h(\frac{\pi}{4})(1-\frac{\pi}{2}tanh(\frac{\pi}{4})]]}{dz})dz. \qquad (27)$$

The governing equations of equilibrium can be derived from Eq. (25) by integrating the displacement gradients by parts and setting the coefficients δu_0, δv_0, δw_b and δw_s zero separately. Thus one can obtain the equilibrium equations associated with the present shear deformation theory.

$$\begin{aligned}\delta\,u:&\quad \frac{\partial N_x}{\partial x}+\frac{\partial N_{xy}}{\partial y}=0\\ \delta\,v:&\quad \frac{\partial N_{xy}}{\partial x}+\frac{\partial N_y}{\partial y}=0\\ \delta\,w_b:&\quad \frac{\partial^2 M_x^b}{\partial x^2}+2\frac{\partial^2 M_{xy}^b}{\partial x\partial y}+\frac{\partial^2 M_y^b}{\partial y^2}+q=0\\ \delta\,w_s:&\quad \frac{\partial^2 M_x^s}{\partial x^2}+2\frac{\partial^2 M_{xy}^s}{\partial x\partial y}+\frac{\partial^2 M_y^s}{\partial y^2}+\frac{\partial S_{xz}^s}{\partial x}+\frac{\partial S_{yz}^s}{\partial y}+q=0\end{aligned} \qquad (28)$$

Using Eq. (22) in Eq. (26), the stress resultants of a plate made up of three layers can be related to the total strains by

$$\begin{Bmatrix}N\\ M^b\\ M^s\end{Bmatrix}=\begin{bmatrix}A & B & B^s\\ A & D & D^s\\ B^s & D^s & H^s\end{bmatrix}\begin{Bmatrix}\varepsilon\\ k^b\\ k^s\end{Bmatrix}, \qquad (29a)$$

$$S=A^s\gamma, \qquad (29b)$$

where

$$N=\left\{N_x,N_y,N_{xy}\right\}^t,\;M^b=\left\{M_x^b,M_y^b,M_{xy}^b\right\}^t,\quad M^s=\left\{M_x^s,M_y^s,M_{xy}^s\right\}^t, \qquad (30a)$$

$$\varepsilon=\left\{\varepsilon_x^0,\varepsilon_y^0,\gamma_{xy}^0\right\}^t,\;k^b=\left\{k_x^b,k_y^b,k_{xy}^b\right\}^t,\quad k^s=\left\{k_x^s,k_y^s,k_{xy}^s\right\}^t, \qquad (30b)$$

$$A=\begin{bmatrix}A_{11} & A_{12} & 0\\ A_{12} & A_{22} & 0\\ 0 & 0 & A_{66}\end{bmatrix},\ B=\begin{bmatrix}B_{11} & B_{12} & 0\\ B_{12} & B_{22} & 0\\ 0 & 0 & B_{66}\end{bmatrix}\ D=\begin{bmatrix}D_{11} & D_{12} & 0\\ D_{12} & D_{22} & 0\\ 0 & 0 & D_{66}\end{bmatrix}, \tag{30c}$$

$$B^s=\begin{bmatrix}B^s_{11} & B^s_{12} & 0\\ B^s_{12} & B^s_{22} & 0\\ 0 & 0 & B^s_{66}\end{bmatrix},\ D^s=\begin{bmatrix}D^s_{11} & D^s_{12} & 0\\ D^s_{12} & D^s_{22} & 0\\ 0 & 0 & D^s_{66}\end{bmatrix}\ H^s=\begin{bmatrix}H^s_{11} & H^s_{12} & 0\\ H^s_{12} & H^s_{22} & 0\\ 0 & 0 & H^s_{66}\end{bmatrix}, \tag{30e}$$

$$S=\left\{S^s_{xz},S^s_{yz}\right\}^t,\ \gamma=\left\{\gamma_{xz},\gamma_{yz}\right\}^t,\quad A^s=\begin{bmatrix}A^s_{44} & 0\\ 0 & A^s_{55}\end{bmatrix}, \tag{30d}$$

where A_{ij}, B_{ij}, etc., are the plate stiffness, defined by

$$\begin{Bmatrix}A_{11} & B_{11} & D_{11} & B^s_{11} & D^s_{11} & H^s_{11}\\ A_{12} & B_{12} & D_{12} & B^s_{12} & D^s_{12} & H^s_{12}\\ A_{66} & B_{66} & D_{66} & B^s_{66} & D^s_{66} & H^s_{66}\end{Bmatrix}=\int_{-\hbar/2}^{\hbar/2} Q_{11}(1,z,z^2,f(z),z\,f(z),f^2(z))\begin{Bmatrix}1\\ \nu\\ \frac{1-\nu}{2}\end{Bmatrix}dz, \tag{31a}$$

and

$$(A_{22},B_{22},D_{22},B^s_{22},D^s_{22},H^s_{22})=(A_{11},B_{11},D_{11},B^s_{11},D^s_{11},H^s_{11}) \tag{31b}$$

$$A^s_{44}=A^s_{55}=\int_{\hbar_{n-1}}^{\hbar_n} Q_{44}[g(z)]^2dz, \tag{31c}$$

Substituting from Eq. (28) into Eq. (29), we obtain the following equation

$$\begin{aligned}A_{11}d_{11}u_0+A_{66}d_{22}u_0+(A_{12}+A_{66})d_{12}v_0-B_{11}d_{111}w_b-(B_{12}+2B_{66})d_{122}w_b\\ -(B^s_{12}+2B^s_{66})d_{122}w_s-B^s_{11}d_{111}w_s=0,\end{aligned} \tag{32a}$$

$$\boldsymbol{\begin{aligned}A_{22}d_{22}v_0+A_{66}d_{11}v_0+(A_{12}+A_{66})d_{12}u_0-B_{22}d_{222}w_b-(B_{12}+2B_{66})d_{112}w_b\\ -(B^s_{12}+2B^s_{66})d_{112}w_s-B^s_{22}d_{222}w_s=0,\end{aligned}} \tag{32b}$$

$$\begin{aligned}B_{11}d_{111}u_0+(B_{12}+2B_{66})d_{122}u_0+(B_{12}+2B_{66})d_{112}v_0+B_{22}d_{222}v_0-D_{11}d_{1111}w_b-\\ -2(D_{12}+2D_{66})d_{1122}w_b-D_{22}d_{2222}w_b-D^s_{11}d_{1111}w_s-2(D^s_{12}+2D^s_{66})d_{1122}w_s\\ -D^s_{22}d_{2222}w_s=q\end{aligned} \tag{32c}$$

$$\begin{aligned}B^s_{11}d_{111}u_0+(B^s_{12}+2B^s_{66})d_{122}u_0+(B^s_{12}+2B^s_{66})d_{112}v_0+B^s_{22}d_{222}v_0-\\ -D^s_{11}d_{1111}w_b-2(D^s_{12}+2D^s_{66})d_{1122}w_b-D^s_{22}d_{2222}w_b-H^s_{11}d_{1111}w_s-\\ -2(H^s_{12}+2H^s_{66})d_{1122}w_s-H^s_{22}d_{2222}w_s+A^s_{55}d_{11}w_s+A^s_{44}d_{22}w_s=q\end{aligned} \tag{32d}$$

Where d_{ij}, d_{ijl} and d_{ilmj} are the following differential operators:

$$d_{ij}=\frac{\partial^2}{\partial x_i\partial x_j},\ d_{ijl}=\frac{\partial^3}{\partial x_i\partial x_j\partial x_l},\ d_{ijlm}=\frac{\partial^4}{\partial x_i\partial x_j\partial x_l\partial x_m},\ d_i=\frac{\partial}{\partial x_i},\ (i,j,l,m=1,2). \tag{33}$$

2.2.4 Exact solutions for FGMs plates

The exact solution of Eq. (32) for the FGM plate under various boundary conditions can be constructed. The boundary conditions for an arbitrary edge with simply supported and clamped edge conditions are:

Clamped (C)

$$u=v=w_b=w_s=\frac{\partial w_b}{\partial x}=\frac{\partial w_b}{\partial y}=\frac{\partial w_s}{\partial x}=\frac{\partial w_s}{\partial y}=0\ \text{at}\ x=0,a\ \text{and}\ y=0,b \tag{34}$$

Simply supported (S)

Table 2 Admissible functions $X_m(x)$ and $Y_n(y)$

	Boundary conditions		The functions $X_m(x)$ and $Y_n(y)$	
	at x=0, a	at y=0, b	$X_m(x)$	$Y_n(y)$
SSSS	$X_m(0) = X_m^{''}(0) = 0$ $X_m(a) = X_m^{''}(a) = 0$	$Y_n(0) = Y_n^{''}(0) = 0$ $Y_n(b) = Y_n^{''}(b) = 0$	$sin(\lambda x)$	$sin(\mu y)$
CCSS	$X_m(0) = X_m^{'}(0) = 0$ $X_m(a) = X_m^{'}(a) = 0$	$Y_n(0) = Y_n^{''}(0) = 0$ $Y_n(b) = Y_n^{''}(b) = 0$	$sin^2(\lambda x)$	$sin(\mu y)$
CSCS	$X_m(0) = X_m^{'}(0) = 0$ $X_m(a) = X^{''}_m(a) = 0$	$Y_n(0) = Y_n^{''}(0) = 0$ $Y_n(b) = Y_n^{''}(b) = 0$	$sin(\lambda x)\,[cos(\lambda x) - 1]$	$sin(\mu y)\,[cos(\mu y) - 1]$
CCCC	$X_m(0) = X_m^{'}(0) = 0$ $X_m(a) = X_m^{'}(a) = 0$	$Y_n(0) = Y_n^{'}(0) = 0$ $Y_n(b) = Y_n^{'}(b) = 0$	$sin^2(\lambda x)$	$sin^2(\mu y)$

$$\begin{cases} v = w_b = w_s = \dfrac{\partial w_b}{\partial y} = \dfrac{\partial w_s}{\partial y} = 0 \text{ at } x = 0, a \\ u = w_b = w_s = \dfrac{\partial w_b}{\partial x} = \dfrac{\partial w_s}{\partial x} = 0 \text{ at } y = 0, b \end{cases} \tag{35}$$

The following representation for the displacement quantities, that satisfy the above boundary conditions, is appropriate in the case of our problem, Then the boundary conditions in Eq. (34) and (35) are satisfied by the following expansions

$$\begin{Bmatrix} u_0 \\ v_0 \\ w_b \\ w_s \end{Bmatrix} = \sum_{m=1}^{\infty}\sum_{n=1}^{\infty} \begin{Bmatrix} U_{mn} X_m^{'}(x) Y_n(y) \\ V_{mn} X_m(x) Y_n^{'}(y) \\ W_{bmn} X_m(x) Y_n(y) \\ W_{smn} X_m(x) Y_n(y) \end{Bmatrix} \tag{36}$$

where U_{mn}, V_{mn}, W_{bmn} and W_{smn} unknown parameters that should be determined, Eigen-mode and ()' denotes the derivative with respect to the corresponding coordinate. The functions $X_m(x)$ and $Y_n(x)$ are proposed to satisfy at least the geometric boundary conditions given in Eqs. (34) and (35) and represent he approximate shapes of the deflected surface of the plate. These functions are listed in Table 2 for the different boundary conditions cases with $\lambda = m\pi/a$ and $\mu = n\pi/b$.

Substituting Eqs. (36) and (32) into Eq. (31), the exact solution of FGM plate can be determined from the following equations:

$$\begin{bmatrix} a_{11} & a_{12} & a_{13} & a_{14} \\ a_{21} & a_{22} & a_{23} & a_{24} \\ a_{31} & a_{32} & a_{33} & a_{34} \\ a_{41} & a_{42} & a_{43} & a_{44} \end{bmatrix} \begin{Bmatrix} U_{mn} \\ V_{mn} \\ W_{bmn} \\ W_{smn} \end{Bmatrix} = \begin{Bmatrix} 0 \\ 0 \\ -q \\ -q \end{Bmatrix} \tag{37}$$

where

$$a_{11} = \int_0^a \int_0^b \left(A_{11} X_m^{'''} Y_n + A_{66} X_m^{'} Y_n^{''}\right) X_m^{'} Y_n \, dxdy \tag{38a}$$

$$a_{12} = \int_0^a \int_0^b (A_{12} + A_{66})\, X_m^{'} Y_n^{''} X_m^{'} Y_n \, dxdy \tag{38b}$$

$$a_{13} = -\int_0^a \int_0^b \left[B_{11} X_m^{''} Y_n + (B_{12} + 2B_{66}) X_m^{'} Y_n^{''}\right] X_m^{'} Y_n \, dxdy \tag{38c}$$

$$a_{14} = -\int_0^a \int_0^b \left[B_{11}^s X_m^{''} Y_n + (B_{12}^s + 2B_{66}^s) X_m^{'} Y_n^{''}\right] X_m^{'} Y_n \, dxdy \tag{38d}$$

$$a_{21} = \int_0^a \int_0^b (A_{12} + A_{66})\, X_m'' Y_n' X_m Y_n' dxdy \tag{38e}$$

$$a_{22} = \int_0^a \int_0^b \left(A_{22} X_m Y_n''' + A_{66} X_m'' Y_n'\right) X_m Y_n' dxdy \tag{38f}$$

$$a_{23} = -\int_0^a \int_0^b \left[B_{22} X_m Y_n''' + (B_{12} + 2B_{66}) X_m'' Y_n'\right] X_m Y_n' dxdy \tag{38g}$$

$$a_{24} = -\int_0^a \int_0^b \left[B_{22}^s X_m Y_n''' + (B_{12}^s + 2B_{66}^s) X_m'' Y_n'\right] X_m Y_n' dxdy \tag{38h}$$

$$a_{31} = \int_0^a \int_0^b \left[B_{11} X_m'''' Y_n + (B_{12} + 2B_{66}) X_m'' Y_n''\right] X_m Y_n dxdy \tag{38i}$$

$$a_{32} = \int_0^a \int_0^b \left[B_{22} X_m Y_n'''' + (B_{12} + 2B_{66}) X_m'' Y_n''\right] X_m Y_n dxdy \tag{38j}$$

$$a_{33} = \int_0^a \int_0^b -\left[D_{11} X_m'''' Y_n + 2(D_{12} + 2D_{66}) X_m'' Y_n'' + D_{22} X_m Y_n''''\right] X_m Y_n dxdy \tag{38k}$$

$$a_{34} = \int_0^a \int_0^b -\left[D_{11}^s X_m'''' Y_n + 2(D_{12}^s + 2D_{66}^s) X_m'' Y_n'' + D_{22}^s X_m Y_n''''\right] X_m Y_n dxdy \tag{38l}$$

$$a_{41} = \int_0^a \int_0^b \left[B_{11}^s X_m'''' Y_n + (B_{12}^s + 2B_{66}^s) X_m'' Y_n''\right] X_m Y_n dxdy \tag{38m}$$

$$a_{42} = \int_0^a \int_0^b \left[B_{22}^s X_m Y_n'''' + (B_{12}^s + 2B_{66}^s) X_m'' Y_n''\right] X_m Y_n dxdy \tag{38n}$$

$$a_{43} = \int_0^a \int_0^b -\left[D_{11}^s X_m'''' Y_n + 2(D_{12}^s + 2D_{66}^s) X_m'' Y_n'' + D_{22}^s X_m Y_n''''\right] X_m Y_n dxdy \tag{38o}$$

$$a_{44} = \int_0^a \int_0^b -\begin{bmatrix} H_{11}^s X_m'''' Y_n + 2(H_{12}^s + 2H_{66}^s) X_m'' Y_n'' + H_{22}^s X_m Y_n'''' \\ -A_{55}^s X_m'' Y_n - A_{44}^s X_m Y_n'' \end{bmatrix} X_m Y_n dxdy \tag{38p}$$

$$m_{11} = \int_0^a \int_0^b -I_1\, X_m' Y_n X_m' Y_n dxdy \tag{38p}$$

$$m_{11} = \int_0^a \int_0^b -I_1\, X_m' Y_n X_m' Y_n dxdy \tag{38q}$$

3. Presentation and analysis of results

In numerical analysis, the deflections and stresses of perfect and imperfect FG plates with various boundary conditions are evaluated. The FG plate is taken to be made of aluminum and alumina with the following material properties:

- Ceramic (P_C: Alumina, Al_2O_3): E_c = 380 GPa;

Table 3 Maximum dimensionless deflections of homogeneous rectangular FG plates under uniform loads for different case of porosity distribution rate

Method	*a* = *b*			*a* = 0.5*b*		
	a/h = 25	10	5	*a/h* = 25	10	5
Reddy *et al*.	0.410	0.427	0.490	1.018	1.045	1.043
Cooke and Levinson	0.410	0.427	0.490	1.018	1.045	1.043
Lee *et al*.	0.410	0.427	0.490	1.018	1.045	1.043
Zenkour and Radwan	0.40960	0.427	0.490	1.018	1.045	1.043
Present: Type-I	0.4096	0.4272	0.4901	1.0180	1.0453	1.1427

Table 4 Comparison of normalized displacements and stresses of porous FGM rectangular plate for different case of porosity distribution rate (b = 3a, k = 2, α =0.2)

a/h	Theory		w	σ_x	σ_y	τ_{yz}	τ_{xz}	τ_{xy}
4	Karama (2003)-ESDPT α=0		4.0569	5.2804	0.6644	0.6084	0.6699	0.5900
	Tounsi (2013)-PSDPT α=0		4.0529	5.2759	0.6652	0.6058	0.6545	0.5898
	Benferhat (2016a) α=0		3.8716	5.4197	0.66778	0.6096	0.6802	0.5395
	Benferhat (2016a) α=0.2		6.2567	6.8649	0.6809	0.6598	0.6624	0.4148
	Present theory	Type-I α=0	3.8716	5.4197	0.66778	0.6096	0.6802	0.5395
		Type-II α=0.2	6.2567	6.8649	0.6809	0.6598	0.6624	0.4148
		Type-III α=0.2	3.9236	7.2661	0.6992	0.6956	0.7045	0.4656
		Type-IV α=0.2	5.7275	6.5461	0.6635	0.6272	0.6268	0.3734
		Type-V α=0.2	5.1509	6.1977	0.7008	0.6681	0.7126	0.3248
		Type-VI α=0.2	5.1068	6.1710	0.6389	0.5836	0.5809	0.3248
10	Karama (2003)-ESDPT α=0		3.5543	12.9252	1.6938	0.61959	0.6841	1.4898
	Tounsi (2013)-PSDPT α=0		3.5537	12.9234	1.6941	0.6155	0.6672	1.4898
	Present theory	Type-I α=0	3.5231	12.9841	1.6995	0.6211	0.6922	1.4659
		Type-II α=0.2	5.992	16.6660	1.7174	0.6723	0.6679	1.1948
		Type-III α=0.2	6.7275	17.7296	1.7663	0.7088	0.7057	1.3692
		Type-IV α=0.2	5.4310	15.8318	1.6712	0.6391	0.6340	1.0605
		Type-V α=0.2	4.7770	14.8653	1.6066	0.5947	0.5892	0.9084
		Type-VI α=0.2	8.3196	20.0399	1.7625	0.7701	0.7727	1.7563
20	Karama (2003)-ESDPT α=0		3.4824	25.7712	3.3971	0.6214	0.6878	2.9844
	Tounsi (2013)-PSDPT α=0		3.48225	25.7703	3.3972	0.6171	0.6704	2.9844
	Present theory	Type-I α=0	3.4745	25.8012	3.4001	0.6231	0.6951	2.9719
		Type-II α=0.2	5.9665	33.1876	3.4388	0.6745	0.6687	2.4428
		Type-III α=0.2	6.7046	35.3343	3.5375	0.7111	0.7054	2.8057
		Type-IV α=0.2	5.3920	31.5074	3.3457	0.6412	0.6354	2.1644
		Type-V α=0.2	4.7324	29.5652	3.2154	0.59672	0.5909	1.8498
		Type-VI α=0.2	8.3231	40.0105	3.6969	0.77259	0.7679	3.0176

- Metal (P_M: Aluminium, Al): E_m = 70 GPa; v = 0.3;

And their properties change through the thickness of the plate according to power-law. The bottom surfaces of the FG plate are aluminum rich, whereas the top surfaces of the FG plate are alumina rich.

To validate accuracy of the results, the comparisons between the present theory and the available results obtained by Reddy *et al*., Cooke and Levinson, Lee *et al*. and Zenkour and Radwan in Table 3. The present solution is realized for maximum dimensionless deflections of homogeneous rectangular FG plates under uniform loads. It is to be noted that the present results of the deflection and stresses compare very well with the other theories solution for perfect FG plate.

For the sake of comparison, some results are tabulated here for comparison with the available ones in the literature. Tables 4 and 5 shows the normalized displacements and stresses of SSSS porous rectangular plates for different case of porosity distribution rate according to uniform loads (k_0=k_1=0). the plate is viewed as rectangular b=3a. It is to be noted that the present results of the deflection and stresses compare very well with the other theories solution for perfect FG plate (α=0). We can also note that the variation in the porosity distribution rate has a significant effect in the

Table 5 Dimensionless deflections and stresses of rectangular plates under uniform loads for different case of porosity distribution rate α =0.2, a=10h, b=3a

p	Method		w^*	σ_x^*	σ_y^*	σ_{xy}^*
2	Zenkour (2009)		3.2267	0.4396	0.1502	0.1766
	Thai (2013)		3.2266	0.4395	0.1502	0.1766
	Present	Type-I	3.2267	0.4395	0.1522	0.1766
		Type-II	5.4793	0.2892	0.0998	0.1159
		Type-III	6.1361	0.2474	0.0853	0.0990
		Type-IV	4.9649	0.3224	0.1114	0.1292
		Type-V	7.5609	0.1581	0.0545	0.0632
		Type-VI	4.37074	0.3615	0.1250	0.1450

Table 6 Effects of parameter b on the deflections w of simply-supported FG square plates under sinusoidal loads for different case of porosity distribution rate. α=0.2

p	a/h	Method								
		Zenkour (2018)	Tounsi (2013)	Thai (2013)	Present					
					Type-I	Type-II	Type-III	Type-IV	Type-V	Type-VI
1	4	0.7284	0.7020	0.7304	0.7282	0.9933	1.0486	0.9442	1.1464	0.8801
	10	0.5889	0.5868	0.5913	0.5889	0.8192	0.86834	0.7759	0.9560	0.7198
	100	0.5625	0.5648	0.5649	0.5625	0.7862	0.8341	0.7440	0.9199	0.6894
4	4	1.1573	1.1108	1.1644	1.1614	2.2304	2.6230	1.9549	3.7150	1.6635
	10	0.8810	0.8700	0.8844	0.8844	1.7658	2.1147	1.5282	3.1333	1.2840
	100	0.8287	0.8240	0.8312	0.8312	1.6776	2.0181	1.4471	3.0227	1.2119
10	4	1.3889	1.3334	1.3953	1.3953	3.0206	3.7234	2.5638	6.0729	2.1100
	10	1.0083	0.9888	1.0132	1.0132	2.1234	2.6177	1.8082	4.3778	1.4985
	100	0.9362	0.9227	0.9406	0.9406	1.9527	2.4072	1.6645	4.0543	1.3823

Table 7 Dimensionless transverse displacement of FGM square plate subjected to uniform load for different case of porosity distribution rate. α=0.2, P=1

E_C/E_M	a/h	Method								
		Abdelaziz (2017)	Tounsi (2013)	Quasi-3D Adim (2018)	Present					
					Type-I	Type-II	Type-III	Type-IV	Type-V	Type-VI
0.5	0.2	8.9751	9.0047	8.8724	9.6097	12.0165	11.8398	12.1986	11.5843	12.4823
1	0.2	12.5997	12.6134	12.5970	13.6780	17.0975	17.0975	17.0975	17.0975	17.0975
2	0.2	17.6640	17.1718	17.1718	17.7633	22.2124	22.5489	21.8857	23.0733	21.4134

bending and stresses.

Tables 6 and 7 shows the effect of the type of loading and the variation in the porosity distribution rate in the deflection of SSSS FG square plates. The present theory gives excellent results for side-to-thickness a/h ratios as well as for the FG parameter P. We can see that the deflection becomes larger when the porosity rate is higher in the ceramic. The deflection increases as the FG parameter P increases.

Table 7 present a comparison study of nondimensionalized deflection of FG square plates resting on elastic foundations under sinusoidal loads. The power law index varied from 1 to 10. The

Table 8 Nondimensionalized deflection w of FG square plates resting on elastic foundations under sinusoidal loads $(a = 10h, \alpha = 0.2)$ (Al/Al_2O_3)

k_0	k_1	Theory		k			
				1	2	5	10
0	0	Ameur *et al.* (2009)		0.5889	0.7573	0.9118	1.0089
		Tounsi (2013)		0.5680	0.7198	0.8725	0.9807
		Present	Type-I	0.5889	0.7573	0.9117	1.0088
			Type-II	0.8192	1.2800	1.8754	2.1234
			Type-III	0.8683	1.4317	2.2782	2.6177
			Type-IV	0.7759	1.1610	1.6091	1.8082
			Type-V	0.9560	1.7602	3.5522	4.3778
			Type-VI	0.7198	1.0233	1.3415	1.4985
100	0	Ameur *et al.* (2011)		0.3825	0.4471	0.4969	0.5244
		Tounsi (2013)		0.3747	0.4352	0.4867	0.5189
		Present	Type-I	0.3825	0.4471	0.4968	0.5243
			Type-II	0.4680	0.5892	0.6901	0.7211
			Type-III	0.4837	0.6195	0.7381	0.7705
			Type-IV	0.4536	0.5627	0.6505	0.6808
			Type-V	0.5097	0.6739	0.8352	0.8739
			Type-VI	0.4338	0.5282	0.6019	0.6316
100	10	Ameur *et al.* (2011)		0.2261	0.2472	0.2617	0.2692
		Tounsi (2013)		0.2241	0.2444	0.2599	0.2689
		Present	Type-I	0.2261	0.2472	0.2617	0.2692
			Type-II	0.2535	0.2853	0.3070	0.3130
			Type-III	0.2580	0.2922	0.3162	0.3220
			Type-IV	0.2492	0.2789	0.2989	0.3052
			Type-V	0.2652	0.3038	0.3327	0.3387
			Type-VI	0.2431	0.2702	0.2882	0.2949

nondimensionalized deflection is calculated with 6 types of rule of mixture. It is to be noted that the present results of the deflection (type-I) compare very well with the ones of Ameur *et al.* (2011) and Zenkour *et al* (2014) of FGM plate with and without elastic foundation. We can see that the deflection is maximum when the pore distribution is of type-V.

For the sake of completeness, additional results for the effect of the variation in the porosity distribution rate on the deflections are presented in Tables 9 and 10. Table 8 shows the deflection of FG plates under uniform loads (k_0=k_1=0) while Table 8 shows the deflection of FG plates resting on Winkler-Pasternak foundation (k_0=k_1=10). Different boundary conditions as well as different values of the side-to-thickness ratio a/h are used in these tables. With the increase of the side-to-thickness ratio a/h a decrement for deflection can be clearly observed. The CCCC FG plate gives the largest deflections while the SSSS FG plate gives the smallest ones.

The dimensionless center deflection as function of the aspect ratio (*a/b*) and side-to-thickness ratio (*a/h*) of porous FGM plate for different variation of porosity distribution rate are illustrated in Figs. 2 and 3, respectively. The gradient index is taken equal to *P*=10. The FGM plate is considered without an elastic foundation (a), reposed on winkler foundation (b) and reposed on winkler-

Table 9 Dimensionless deflections w of FG square plates according to various boundary conditions without elastic foundations for different case of porosity distribution rate. P=10

a/h	Method present	Boundary conditions		
		SSSS	CSCS	CCCC
10	Type-I	1.5874	1.6400	1.7105
	Type-II	2.1019	2.1724	2.2672
	Type-III	2.2063	2.2805	2.3802
	Type-IV	2.0084	2.0757	2.1660
	Type-V	2.3888	2.4693	2.5777
	Type-VI	1.8851	1.9480	2.0326
100	Type-I	1.4817	1.5194	1.5663
	Type-II	1.9539	2.0036	2.0655
	Type-III	2.0497	2.1018	2.1668
	Type-IV	1.8682	1.9157	1.9749
	Type-V	2.2170	2.2754	2.3437
	Type-VI	1.7551	1.7997	1.8553

Table 10 Dimensionless deflections w of FG square plates according to various boundary conditions with elastic foundations for different case of porosity distribution rate. K_0=K_1=10, P=10

a/h	Present method	Boundary conditions		
		SSSS	CSCS	CCCC
10	Type-I	0.5290	0.5646	0.6141
	Type-II	0.5741	0.6171	0.6777
	Type-III	0.5813	0.6256	0.6882
	Type-IV	0.5672	0.6090	0.6677
	Type-V	0.5926	0.6392	0.7052
	Type-VI	0.5573	0.5974	0.6536
100	Type-I	0.5200	0.5479	0.5837
	Type-II	0.5665	0.6004	0.6443
	Type-III	0.5739	0.6090	0.6544
	Type-IV	0.5593	0.5922	0.6347
	Type-V	0.5858	0.6227	0.6707
	Type-VI	0.5491	0.5806	0.6212

pasternak foundation (c). It can be seen that the deflection decreases as the aspect ratio a/b and the side-to-thickness ratio a/h increase. Also, the case of FG plate without elastic foundation gives the largest deflection. The type-V of the variation in the porosity distribution rate in FG plate gives the largest deflections while the type-I gives the smallest ones.

The effect of the variation of porosity distribution rate on the in-plane longitudinal stress σ_{xx} and in the in-plane normal stress σ_{yy} through-the thickness of porous FGM plate subjected to uniform distribution load is shown in Figs. 4 and 5, respectively. As it can be seen, the in-plane normal and longitudinal stresses are more important in the case of FG plate without elastic foundation. It can also be noted that the variation in the porosity distribution rate has a considerable effect on the stresses.

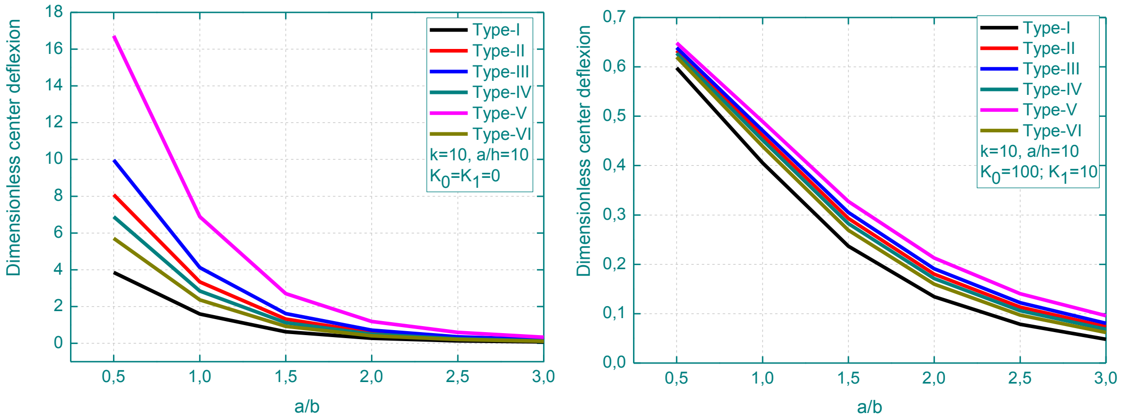

Fig. 2 Dimensionless center deflection (w) as function of the aspect ratio (a/b) of porous FGM plate for different case of porosity distribution rate

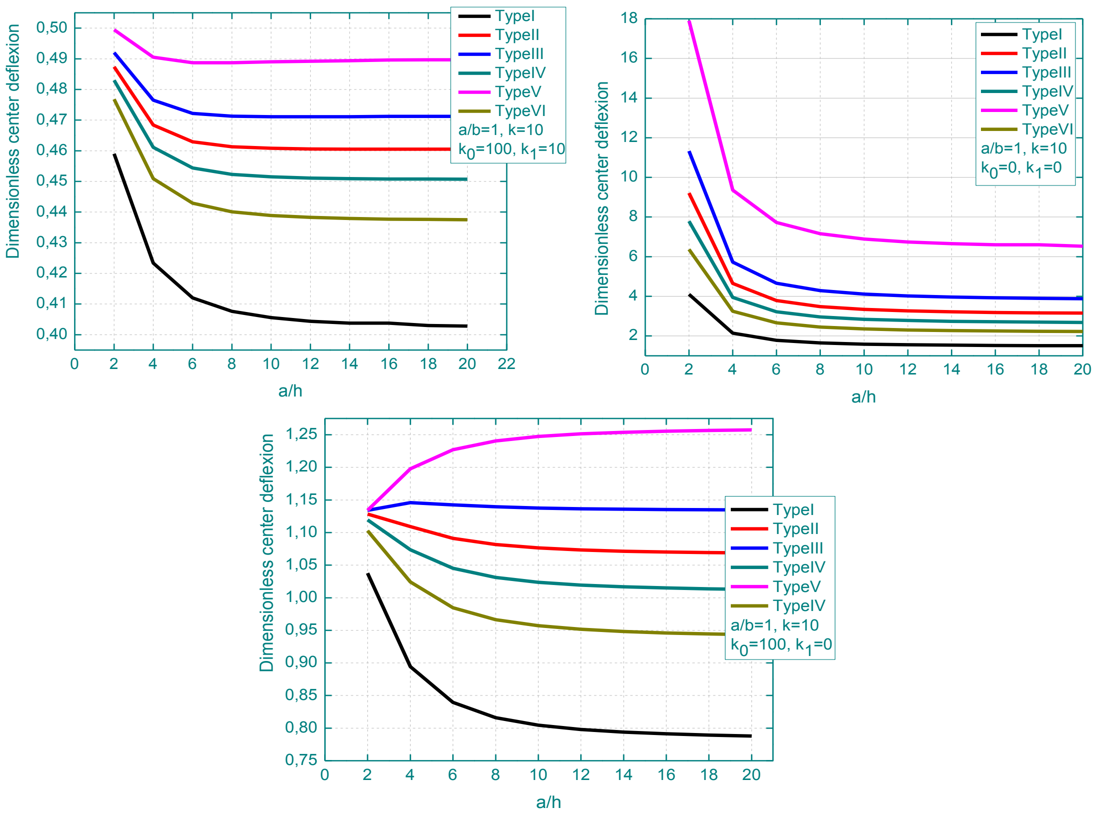

Fig. 3 Dimensionless center deflection (w) as a function of the side-to-thickness ratio (a/h) of porous FGM square plate for different case of porosity distribution rate

Fig. 6 display the variation In plane shear stresses σ_{xy} through-the thickness of an FGM plate for different case of porosity distribution rate. The gradient index is taken equal P=10. The side-to-thickness ratio is considered equal *a/h*=10. it can be observed that the effect of the variation of the porosity distribution rate on the stresses becomes more important in the case of FGM plates resting on a Winkler or Winkler-pasternak type foundation.

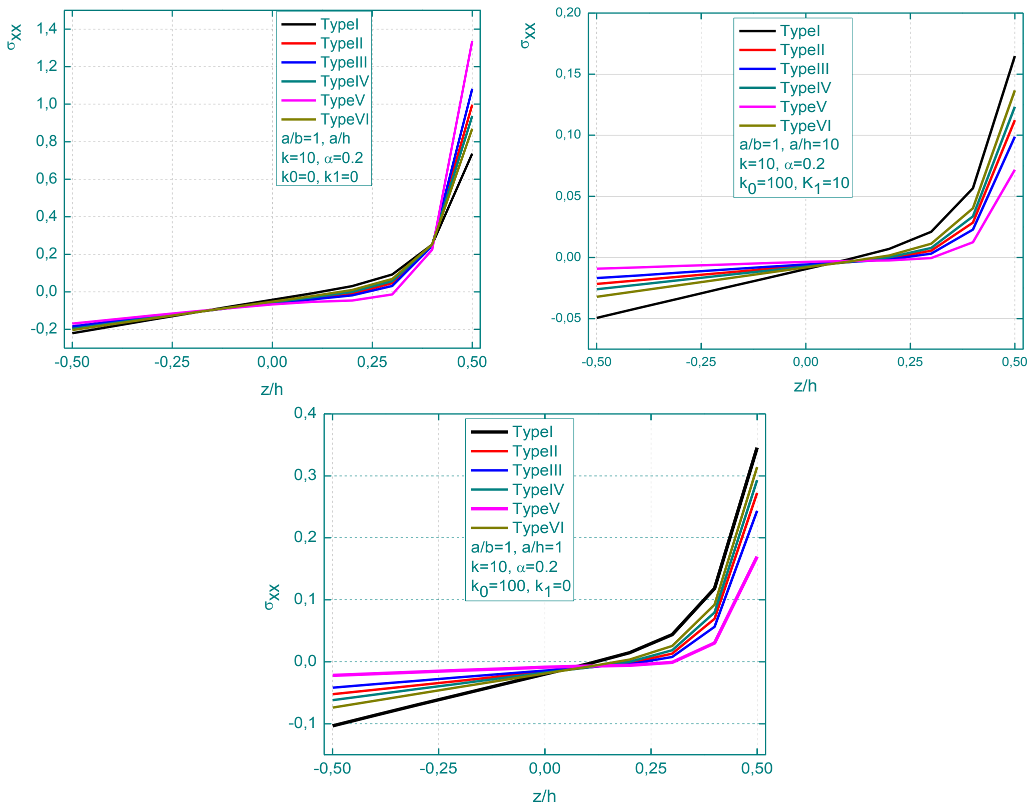

Fig. 4 Variation of in-plane longitudinal stress σ_{xx} through-the thickness of porous FGM plate for different case of porosity distribution rate

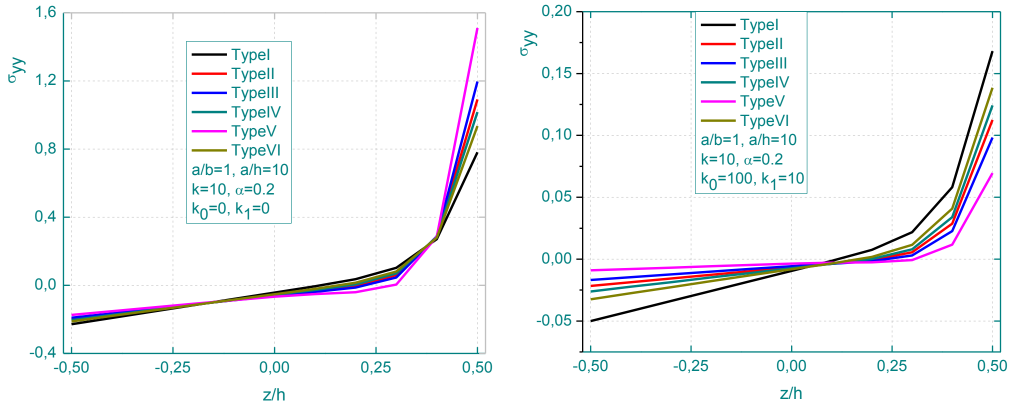

Fig. 5 Variation of in-plane normal stress σ_{yy} through-the thickness of porous FGM plate for different case of porosity distribution rate

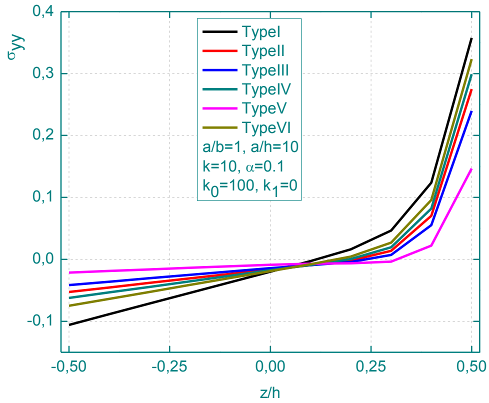

Fig. 5 Continued

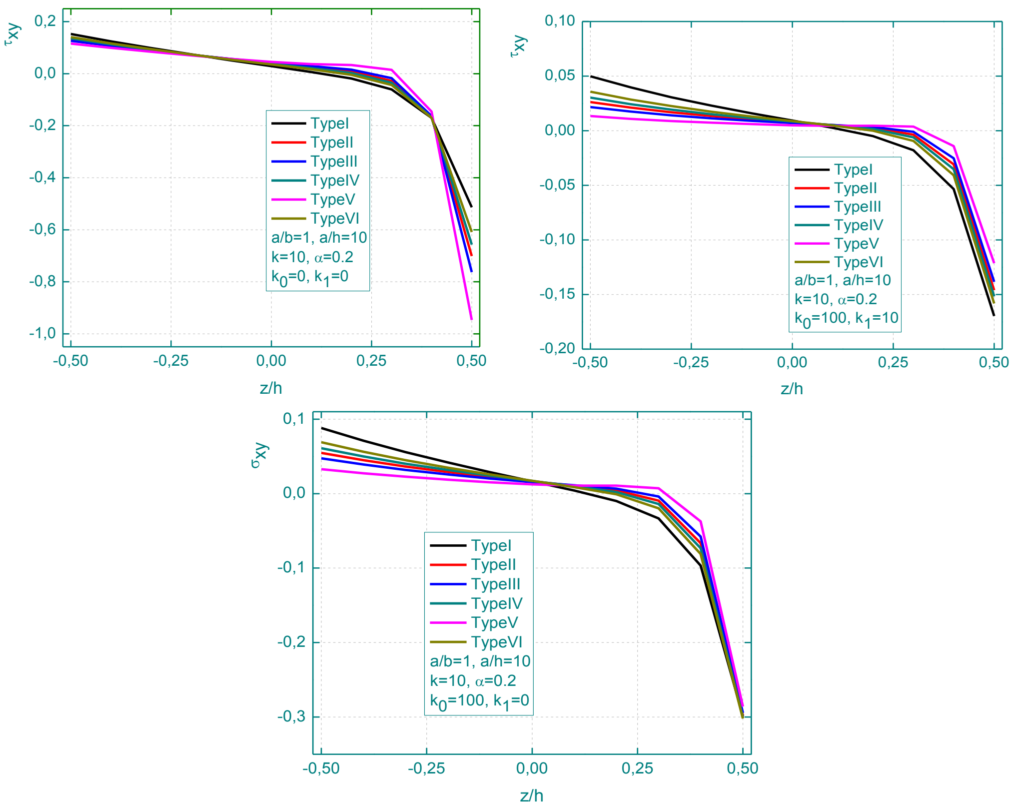

Fig. 6 Variation of In plane shear stresses σ_{xy} through-the thickness of an FGM plate for different case of porosity distribution rate

4. Conclusions

In this paper, a new refined shear deformation theory is used for the bending response of porous FG plates resting on Winkler-Pasternak foundation. The bending analysis is presented here for FG plates subjected uniform and sinusoidal loads with three different boundary conditions. The present model satisfies the zero shear stresses on the lower and upper surfaces of the plate without requiring any shear correction factors. The modified rule of mixture covering different variation of porosity distribution rate is used to describe and approximate material properties of the imperfect FG plates. The results have been included the effects of the variation of porosity distribution rate and elastic foundations parameters as well as different boundary conditions. It is clear that the present theory gives results that compared well with the available ones in the literature. The effect of the variation in the porosity distribution rate is demonstrated. Numerical examples show that the proposed theory gives solutions which are almost identical with those obtained using other shear deformation theories.

Acknowledgments

This research was supported by the Algerian Ministry of Higher Education and Scientific Research (MESRS) as part of the grant for the PRFU research project n° A01L02UN140120200002 and by the University of Tiaret, in Algeria.

References

Abdelaziz, H.H., Meziane, M.A.A., Bousahla, A.A., Tounsi, A., Mahmoud, S.R. and Alwabli, A.S. (2017), "An efficient hyperbolic shear deformation theory for bending, buckling and free vibration of FGM sandwich plates with various boundary conditions", *Steel Compos. Struct.*, **25**(6), 693-704. https://doi.org/10.12989/scs.2017.25.6.693.

Abdelhak, Z., Hadji, L., Khelifa, Z., Hassaine Daouadji, T. and Adda Bedia, E.A. (2016), "Analysis of buckling response of functionally graded sandwich plates using a refined shear deformation theory", *Wind Struct.*, **22**(3), 291-305. https://doi.org/10.12989/was.2016.22.3.291.

Abderezak, R., Daouadji, T.H. and Rabia, B. (2020), "Analysis of interfacial stresses of the reinforced concrete foundation beams repairing with composite materials plate", *Coupl. Syst. Mech.*, **9**(5), 473-498. http://dx.doi.org/10.12989/csm.2020.9.5.473.

Abderezak, R., Daouadji, T.H., Rabia, B. and Belkacem, A. (2018), "Nonlinear analysis of damaged RC beams strengthened with glass fiber reinforced polymer plate under symmetric loads", *Earthq. Struct.*, **15**(2), 113-122. https://doi.org/10.12989/eas.2018.15.2.113.

Abderezak, R., Rabia, B., Daouadji, T.H., Abbes, B., Belkacem, A. and Abbes, F. (2019), "Elastic analysis of interfacial stresses in prestressed PFGM-RC hybrid beams", *Adv. Mater. Res.*, **7**(2), 83-103. https://doi.org/10.12989/amr.2018.7.2.083.

Abualnour, M., Houari, M.S.A., Tounsi, A. and Mahmoud, S.R. (2018), "A novel quasi-3D trigonometric plate theory for free vibration analysis of advanced composite plates", *Compos. Struct.*, **184**, 688-697. https://doi.org/10.1016/j.compstruct.2017.10.047.

Addou, F.Y., Meradjah, M., Bousahla, A.A., Benachour, A., Bourada, F., Tounsi, A. and Mahmoud, S.R. (2019), "Influences of porosity on dynamic response of FG plates resting on Winkler/Pasternak/Kerr foundation using quasi 3D HSDT", *Comput. Concrete*, **24**(4), 347-367. https://doi.org/10.12989/cac.2019.24.4.347.

Adim, B. and Daouadji, T.H. (2016), "Effects of thickness stretching in FGM plates using a quasi-3D higher order shear deformation theory", *Adv. Mater. Res.*, **5**(4), 223-244. https://doi.org/10.12989/amr.2016.5.4.223.

Ait Atmane, H., Tounsi, A. and Bernard, F. (2015), "Effect of thickness stretching and porosity on mechanical response of a functionally graded beams resting on elastic foundations", *Int. J. Mech. Mater.*, **13**(1), 1-14. https://doi.org/10.1007/s10999-015-9318-x.

Ait Yahia, S., Ait Atmane, H., Houari, M.S.A. and Tounsi, A. (2015), "Wave propagation in functionally graded plates with porosities using various higher-order shear deformation plate theories", *Struct. Eng. Mech.*, **53**(6), 1143-1165. https://doi.org/10.12989/sem.2015.53.6.1143.

Al-Furjan, M.S.H., Habibi, M., Chen, G., Safarpour, H., Safarpour, M. and Tounsi, A. (2020), "Chaotic oscillation of a multi-scale hybrid nano-composites reinforced disk under harmonic excitation via GDQM", *Compos. Struct.*, **252**, 112737. https://doi.org/10.1016/j.compstruct.2020.112737.

Al-Furjan, M.S.H., Safarpour, H., Habibi, M., Safarpour, M. and Tounsi, A. (2020), "A comprehensive computational approach for nonlinear thermal instability of the electrically FG-GPLRC disk based on GDQ method", *Eng. Comput.*, 1-18. https://doi.org/10.1007/s00366-020-01088-7.

Alimirzaei, S., Mohammadimehr, M. and Tounsi, A. (2019), "Nonlinear analysis of viscoelastic micro-composite beam with geometrical imperfection using FEM: MSGT electro-magneto-elastic bending, buckling and vibration solutions", *Struct. Eng. Mech.*, **71**(5), 485-502. https://doi.org/10.12989/sem.2019.71.5.485.

Ameur, M., Tounsi, A., Mechab, I. and Bedia, E.A. (2011), "A new trigonometric shear deformation theory for bending analysis of functionally graded plates resting on elastic foundations", *J. Civil Eng.*, **15**, 1405-1414. https://doi.org/10.1007/s12205-011-1361-z.

Balubaid, M., Tounsi, A., Dakhel, B. and Mahmoud, S.R. (2019), "Free vibration investigation of FG nanoscale plate using nonlocal two variables integral refined plate theory", *Comput. Concrete*, **24**(6), 579-586. https://doi.org/10.12989/cac.2019.24.6.579.

Belabed, Z., Bousahla, A.A., Houari, M.S.A., Tounsi, A. and Mahmoud, S.R. (2018), "A new 3-unknown hyperbolic shear deformation theory for vibration of functionally graded sandwich plate", *Earthq. Struct.*, **14**(2), 103-115. https://doi.org/10.12989/eas.2018.14.2.103.

Belkacem, A., Tahar, H.D., Abderrezak, R., Amine, B.M., Mohamed, Z. and Boussad, A. (2018), "Mechanical buckling analysis of hybrid laminated composite plates under different boundary conditions", *Struct. Eng. Mech.*, **66**(6), 761-769. https://doi.org/10.12989/sem.2018.66.6.761.

Bellal, M., Hebali, H., Heireche, H., Bousahla, A.A., Tounsi, A., Bourada, F., ... & Tounsi, A. (2020), "Buckling behavior of a single-layered graphene sheet resting on viscoelastic medium via nonlocal four-unknown integral model", *Steel Compos. Struct.*, **34**(5), 643-655. https://doi.org/10.12989/scs.2020.34.5.643.

Benchohra, M., Driz, H., Bakora, A., Tounsi, A., Adda Bedia, E.A. and Mahmoud, S.R. (2018), "A new quasi-3D sinusoidal shear deformation theory for functionally graded plates", *Struct. Eng. Mech.*, **65**(1), 19-31. https://doi.org/10.12989/sem.2018.65.1.019.

Benferhat, R., Daouadji, T.H., Mansour, M.S. and Hadji, L. (2016c), "Effect of porosity on the bending and free vibration response of functionally graded plates resting on Winkler-Pasternak foundations", *Earthq. Struct.*, **10**(5), 1429-1449. https://doi.org/10.12989/eas.2016.10.5.1033.

Benferhat, R., Hassaine Daouadji, T., Hadji, L. and Said Mansour, M. (2016), "Static analysis of the FGM plate with porosities", *Steel Compos. Struct.*, **21**(1), 123-136. https://doi.org/10.12989/scs.2016.21.1.123.

Benferhat, R., Hassaine Daouadji, T., Hadji, L. and Said Mansour, M. (2016), "Static analysis of the FGM plate with porosities", *Steel Compos. Struct.*, **21**(1), 123-136. https://doi.org/10.12989/scs.2016.21.1.123.

Benhenni, M.A., Adim, B., Daouadji, T.H., Abbès, B., Abbès, F., Li, Y. and Bouzidane, A. (2019), "A comparison of closed form and finite element solutions for the free vibration of hybrid cross ply laminated plates", *Mech. Compos. Mater.*, **55**(2), 181-194. https://doi.org/10.1007/s11029-019-09803-2.

Benhenni, M.A., Daouadji, T.H., Abbes, B., Abbes, F., Li, Y. and Adim, B. (2019), "Numerical analysis for free vibration of hybrid laminated composite plates for different boundary conditions", *Struct. Eng. Mech.*, **70**(5), 535-549. https://doi.org/10.12989/sem.2019.70.5.535.

Benhenni, M.A., Daouadji, T.H., Abbes, B., Adim, B., Li, Y. and Abbes, F. (2018), "Dynamic analysis for anti-symmetric cross-ply and angle-ply laminates for simply supported thick hybrid rectangular plates", *Adv. Mater. Res.,* **7**(2), 83-103. https://doi.org/10.12989/amr.2018.7.2.119.

Bensattalah, T., Daouadji, T.H., Zidour, M., Tounsi, A. and Bedia, E.A. (2016), "Investigation of thermal and chirality effects on vibration of single walled carbon nanotubes embedded in a polymeric matrix using nonlocal elasticity theories", *Mech. Compos. Mater.*, **52**(4), 555-568. https://doi.org/10.1007/s11029-016-9606-z.

Bensattalah, T., Zidour, M. and Daouadji, T.H. (2018), "Analytical analysis for the forced vibration of CNT surrounding elastic medium including thermal effect using nonlocal Euler-Bernoulli theory", *Adv. Mater. Res.,* **7**(3), 163-174. https://doi.org/10.12989/amr.2018.7.3.163.

Berghouti, H., Adda Bedia, E.A., Benkhedda, A. and Tounsi, A. (2019), "Vibration analysis of nonlocal porous nanobeams made of functionally graded material", *Adv. Nano Res.*, **7**(5), 351-364. https://doi.org/10.12989/anr.2019.7.5.351.

Bouakaz, K., Daouadji, T.H., Meftah, S.A., Ameur, M., Tounsi, A. and Bedia, E.A. (2014), "A numerical analysis of steel beams strengthened with composite materials", *Mech. Compos. Mater.*, **50**(4), 685-696. https://doi.org/10.1007/s11029-014-9435-x.

Boukhlif, Z., Bouremana, M., Bourada, F., Bousahla, A.A., Bourada, M., Tounsi, A. and Al-Osta, M.A. (2019), "A simple quasi-3D HSDT for the dynamics analysis of FG thick plate on elastic foundation", *Steel Compos. Struct.*, **31**(5), 503-516. https://doi.org/10.12989/scs.2019.31.5.503.

Boulefrakh, L., Hebali, H., Chikh, A., Bousahla, A.A., Tounsi, A. and Mahmoud, S.R. (2019), "The effect of parameters of visco-Pasternak foundation on the bending and vibration properties of a thick FG plate", *Geomech. Eng.*, **18**(2), 161-178. https://doi.org/10.12989/gae.2019.18.2.161.

Bourada, F., Bousahla, A.A., Bourada, M., Azzaz, A., Zinata, A. and Tounsi, A. (2019), "Dynamic investigation of porous functionally graded beam using a sinusoidal shear deformation theory", *Wind Struct.*, **28**(1), 19-30. https://doi.org/10.12989/was.2019.28.1.019.

Bourada, F., Bousahla, A.A., Tounsi, A., Bedia, E.A., Mahmoud, S.R., Benrahou, K.H. and Tounsi, A. (2020), "Stability and dynamic analyses of SW-CNT reinforced concrete beam resting on elastic-foundation", *Comput. Concrete*, **25**(6), 485-495. https://doi.org/10.12989/cac.2020.25.6.485

Bousahla, A.A., Bourada, F., Mahmoud, S.R., Tounsi, A., Algarni, A., Bedia, E.A. and Tounsi, A. (2020), "Buckling and dynamic behavior of the simply supported CNT-RC beams using an integral-first shear deformation theory", *Comput. Concrete*, **25**(2), 155-166. https://doi.org/10.12989/cac.2020.25.2.155.

Carrera, E., Brischetto, S., Cinefra, M. and Soave, M. (2011), "Effects of thickness stretching in functionally graded plates and shells", *Compos. Part B*, **42**, 123-133. http://dx.doi.org/10.1016/j.compositesb.2010.10.005.

Chaabane, L.A., Bourada, F., Sekkal, M., Zerouati, S., Zaoui, F.Z., Tounsi, A., ... & Tounsi, A. (2019), "Analytical study of bending and free vibration responses of functionally graded beams resting on elastic foundation", *Struct. Eng. Mech.*, **71**(2), 185-196. https://doi.org/10.12989/sem.2019.71.2.185.

Chedad, A., Daouadji, T.H., Abderezak, R., Belkacem, A., Abbes, B., Rabia, B. and Abbes, F. (2018), "A high-order closed-form solution for interfacial stresses in externally sandwich FGM plated RC beams", *Adv. Mater. Res.,* **6**(4), 317-328. https://doi.org/10.12989/amr.2017.6.4.317.

Chergui, S., Daouadji, T.H., Hamrat, M., Boulekbache, B., Bougara, A., Abbes, B. and Amziane, S. (2019), "Interfacial stresses in damaged RC beams strengthened by externally bonded prestressed GFRP laminate plate: Analytical and numerical study", *Adv. Mater. Res.,* **8**(3), 197-217. https://doi.org/10.12989/amr.2019.8.3.197.

Chikr, S.C., Kaci, A., Bousahla, A.A., Bourada, F., Tounsi, A., Bedia, E.A., ... & Tounsi, A. (2020), "A novel four-unknown integral model for buckling response of FG sandwich plates resting on elastic foundations under various boundary conditions using Galerkin's approach", *Geomech. Eng.*, **21**(5), 471-487. https://doi.org/10.12989/gae.2020.21.5.471.

Cooke, D.W. and Levinson, M. (1983), "Thick rectangular plates-II, the generalized Lévy solution", *Int. J. Mech. Sci*., **25**, 207-215. https://doi.org/10.1016/0020-7403(83)90094-2.

Daouadji, T.H. (2016b), "Theoretical analysis of composite beams under uniformly distributed load", *Adv. Mater. Res.,* **5**(1), 1-9. https://doi.org/10.12989/amr.2016.5.1.001.

Daouadji, T.H. and Adim, B. (2016a), "An analytical approach for buckling of functionally graded plates", *Adv. Mater. Res.,* **5**(3), 141-169. https://doi.org/10.12989/amr.2016.5.3.141.

Daouadji, T.H. and Benferhat, R. (2016), "Bending analysis of an imperfect FGM plates under hygro-thermo-

mechanical loading with analytical validation", *Adv. Mater. Res.,* 5(1), 35-53. https://doi.org/10.12989/amr.2016.5.1.035.
Daouadji, T.H. and Benferhat, R. (2016), "Bending analysis of an imperfect FGM plates under hygro-thermo-mechanical loading with analytical validation", *Adv. Mater. Res.,* **5**(1), 35-53. https://doi.org/10.12989/amr.2016.5.1.035.
Demirhan, P.A. and Taskin, V. (2019), "Bending and free vibration analysis of Levy-type porous functionally graded plate using state space approach", *Compos. Part B: Eng.*, **160**, 661-676. https://doi.org/10.1016/j.compositesb.2018.12.020.
El-Haina, F., Bakora, A., Bousahla, A.A., Tounsi, A. and Mahmoud, S.R. (2017), "A simple analytical approach for thermal buckling of thick functionally graded sandwich plates", *Struct. Eng. Mech.*, **63**(5), 585-595. https://doi.org/10.12989/sem.2017.63.5.585.
Hadj, B., Rabia, B. and Daouadji, T.H. (2019), "Influence of the distribution shape of porosity on the bending FGM new plate model resting on elastic foundations", *Struct. Eng. Mech.*, **72**(1), 823-832. https://doi.org/10.12989/sem.2019.72.1.061.
Hamrat, M., Bouziadi, F., Boulekbache, B., Daouadji, T.H., Chergui, S., Labed, A. and Amziane, S. (2020), "Experimental and numerical investigation on the deflection behavior of pre-cracked and repaired reinforced concrete beams with fiber-reinforced polymer", *Constr. Build. Mater.*, **249**, 1-13. https://doi.org/10.1016/j.conbuildmat.2020.118745.
Hassaine Daouadji, T. (2013), "Analytical analysis of the interfacial stress in damaged reinforced concrete beams strengthened by bonded composite plates", *Strength Mater.*, **45**(5), 587-597. htttps://doi.org/10.1007/s11223-013-9496-4.
Hassaine Daouadji, T. (2017), "Analytical and numerical modeling of interfacial stresses in beams bonded with a thin plate", *Adv. Comput. Des.*, **2**(1), 57-69. https://doi.org/10.12989/acd.2017.2.1.057.
Hassaine Daouadji, T., Rabahi, A., Benferhat, R. and Adim, B. (2019), "Flexural behaviour of steel beams reinforced by carbon fibre reinforced polymer: Experimental and numerical study", *Struct. Eng. Mech.*, **72**(4), 409-419. https://doi.org/10.12989/sem.2019.72.4.409.
Kaddari, M., Kaci, A., Bousahla, A.A., Tounsi, A., Bourada, F., Tounsi, A., ... & Al-Osta, M.A. (2020), "A study on the structural behaviour of functionally graded porous plates on elastic foundation using a new quasi-3D model: Bending and Free vibration analysis", *Comput. Concrete*, **25**(1), 37-57. https://doi.org/10.12989/cac.2020.25.1.037.
Karama, M., Afaq, K.S. and Mistou, S. (2003), "Mechanical behavior of laminated composite beam by the new multi-layered laminated composite structures model with transverse shear stress continuity", *Int. J. Solid. Struct.*, **40**(6), 1525-1546. https://doi.org/10.1016/S0020-7683(02)00647-9.
Karami, B., Janghorban, M. and Tounsi, A. (2019), "Galerkin's approach for buckling analysis of functionally graded anisotropic nanoplates/different boundary conditions", *Eng. Comput.*, **35**, 1297-1316. https://doi.org/10.1007/s00366-018-0664-9.
Khelifa, Z., Hadji, L., Daouadji, T.H. and Bourada, M. (2018), "Buckling response with stretching effect of carbon nanotube-reinforced composite beams resting on elastic foundation", *Struct. Eng. Mech.*, **67**(2), 125-130. https://doi.org/10.12989/sem.2018.67.2.125.
Lee, K.H., Lim, G.T. and Wang, C.M. (2002), "Thick Lévy plates re-visited", *Int. J. Solid. Struct.*, **39**, 127-144. https://doi.org/10.1016/S0020-7683(01)00205-0.
Mantari, J.L., Oktem, A.S. and Soares, C.G. (2012), "A new trigonometric shear deformation theory for isotropic, laminated composite and sandwich plates", *Int. J. Solid. Struct.*, **49**, 43-53. https://doi.org/10.1016/j.ijsolstr.2011.09.008.
Matouk, H., Bousahla, A.A., Heireche, H., Bourada, F., Bedia, E.A., Tounsi, A., ... & Benrahou, K.H. (2020), "Investigation on hygro-thermal vibration of P-FG and symmetricS-FG nanobeam using integral Timoshenko beam theory", *Adv. Nano Res.*, **8**(4), 293-305. https://doi.org/10.12989/anr.2020.8.4.293.
Medani, M., Benahmed, A., Zidour, M., Heireche, H., Tounsi, A., Bousahla, A.A., ... & Mahmoud, S.R. (2019), "Static and dynamic behavior of (FG-CNT) reinforced porous sandwich plate using energy principle", *Steel Compos. Struct.*, **32**(5), 595-610. https://doi.org/10.12989/scs.2019.32.5.595.
Menasria, A., Kaci, A., Bousahla, A.A., Bourada, F., Tounsi, A., Benrahou, K.H., ... & Mahmoud, S.R. (2020),

"A four-unknown refined plate theory for dynamic analysis of FG-sandwich plates under various boundary conditions", *Steel Compos. Struct.*, **36**(3), 355-367. http://dx.doi.org/10.12989/scs.2020.36.3.355.

Mokhtar, Y., Heireche, H., Bousahla, A.A., Houari, M.S.A., Tounsi, A. and Mahmoud, S.R. (2018), "A novel shear deformation theory for buckling analysis of single layer graphene sheet based on nonlocal elasticity theory", *Smart Struct. Syst.*, **21**(4), 397-405. https://doi.org/10.12989/sss.2018.21.4.397.

Rabahi, A., Daouadji, T.H., Abbes, B. and Adim, B. (2016), "Analytical and numerical solution of the interfacial stress in reinforced-concrete beams reinforced with bonded prestressed composite plate", *J. Reinf. Plast. Compos.*, **35**(3) 258-272. https://doi.org/10.1177/0731684415613633.

Rabhi, M., Benrahou, K.H., Kaci, A., Houari, M.S.A., Bourada, F., Bousahla, A.A., ... & Tounsi, A. (2020), "A new innovative 3-unknowns HSDT for buckling and free vibration of exponentially graded sandwich plates resting on elastic foundations under various boundary conditions", *Geomech. Eng.*, **22**(2), 119-132. https://doi.org/10.12989/gae.2020.22.2.119.

Rabia, B., Abderezak, R., Daouadji, T.H., Abbes, B., Belkacem, A. and Abbes, F. (2018), "Analytical analysis of the interfacial shear stress in RC beams strengthened with prestressed exponentially-varying properties plate", *Adv. Mater. Res.*, **7**(1), 29-44. https://doi.org/10.12989/amr.2018.7.1.029.

Rabia, B., Daouadji, T.H. and Abderezak, R. (2019), "Effect of distribution shape of the porosity on the interfacial stresses of the FGM beam strengthened with FRP plate", *Earthq. Struct.*, **16**(5), 601-609. https://doi.org/10.12989/eas.2019.16.5.601.

Rahmani, M.C., Kaci, A., Bousahla, A.A., Bourada, F., Tounsi, A., Bedia, E.A., ... & Tounsi, A. (2020), "Influence of boundary conditions on the bending and free vibration behavior of FGM sandwich plates using a four-unknown refined integral plate theory", *Comput. Concrete*, **25**(3), 225-244. https://doi.org/10.12989/cac.2020.25.3.225.

Reddy, J.N., Wang, C.M., Lim, G.T. and Ng, K.H. (2001), "Bending solutions of Levinson beams and plates in terms of the classical theories", *Int. J. Solid. Struct.*, **38**, 4701-4720. https://doi.org/10.1016/S0020-7683(00)00298-5.

Refrafi, S., Bousahla, A.A., Bouhadra, A., Menasria, A., Bourada, F., Tounsi, A., ... & Tounsi, A. (2020), "Effects of hygro-thermo-mechanical conditions on the buckling of FG sandwich plates resting on elastic foundations", *Comput. Concrete*, **25**(4), 311-325. https://doi.org/10.12989/cac.2020.25.4.311.

Sahla, M., Saidi, H., Draiche, K., Bousahla, A.A., Bourada, F. and Tounsi, A. (2019), "Free vibration analysis of angle-ply laminated composite and soft core sandwich plates", *Steel Compos. Struct.*, **33**(5), 663-679. https://doi.org/10.12989/scs.2019.33.5.663.

Shariati, A., Ghabussi, A., Habibi, M., Safarpour, H., Safarpour, M., Tounsi, A. and Safa, M. (2020), "Extremely large oscillation and nonlinear frequency of a multi-scale hybrid disk resting on nonlinear elastic foundations", *Thin Wall. Struct.*, **154**, 106840. https://doi.org/10.1016/j.tws.2020.106840.

Slimane, M. (2018), "Analysis of bending of ceramic-metal functionally graded plates with porosities using of high order shear theory", *Adv. Eng. Forum*, **30**, 54-70. https://doi.org/10.4028/www.scientific.net/AEF.30.54.

Tahar, H.D., Abderezak, R. and Rabia, B. (2020), "Flexural performance of wooden beams strengthened by composite plate", *Struct. Monit. Mainten.*, **7**(3), 233-259. http://dx.doi.org/10.12989/smm.2020.7.3.233.

Tayeb, B. and Daouadji, T.H. (2020), "Improved analytical solution for slip and interfacial stress in composite steel-concrete beam bonded with an adhesive", *Adv. Mater. Res.*, **9**(2), 133-153. https://doi.org/10.12989/amr.2020.9.2.133.

Thai, H.T. and Choi, D.H. (2013), "Finite element formulation of various four unknown shear deformation theories for functionally graded plates", *Finite Elem. Anal. Des.*, **75**, 50-61. https://doi.org/10.1016/j.finel.2013.07.003.

Tounsi, A., Al-Dulaijan, S.U., Al-Osta, M.A., Chikh, A., Al-Zahrani, M.M., Sharif, A. and Tounsi, A. (2020), "A four variable trigonometric integral plate theory for hygro-thermo-mechanical bending analysis of AFG ceramic-metal plates resting on a two-parameter elastic foundation", *Steel Compos. Struct.*, **34**(4), 511-524. https://doi.org/10.12989/scs.2020.34.4.511.

Tounsi, A., Daouadji, T.H. and Benyoucef, S. (2008), "Interfacial stresses in FRP-plated RC beams: Effect of adherend shear deformations", *Int. J. Adhes. Adhesiv.*, **29**, 313-351.

https://doi.org/10.1016/j.ijadhadh.2008.06.008.

Tounsi, A., Houari, M.S.A. and Benyoucef, S. (2013), “A refined trigonometric shear deformation theory for thermoelastic bending of functionally graded sandwich plates”, *Aerosp. Sci. Technol.*, **24**, 209-220. https://doi.org/10.1016/j.ast.2011.11.009.

Wattanasakulponga, N. and Ungbhakornb, V. (2014), “Linear and non linear vibration analysis of elastically restrained ends FGM beams with porosities”, *Aerosp. Sci. Technol*., **32**(1), 111-120. https://doi.org/10.1016/j.ast.2013.12.002.

Yazid, M., Heireche, H., Tounsi, A., Bousahla, A.A. and Houari, M.S.A. (2018), “A novel nonlocal refined plate theory for stability response of orthotropic single-layer graphene sheet resting on elastic medium”, *Smart Struct. Syst*., **21**(1), 15-25. https://doi.org/10.12989/sss.2018.21.1.015.

Younsi, A., Tounsi, A., Zaoui, F.Z., Bousahla, A.A. and Mahmoud, S.R. (2018), “Novel quasi-3D and 2D shear deformation theories for bending and free vibration analysis of FGM plates”, *Geomech. Eng.*, **14**(6), 519-532. https://doi.org/10.12989/gae.2018.14.6.519.

Zaoui, F.Z., Ouinas, D. and Tounsi, A. (2019), “New 2D and quasi-3D shear deformation theories for free vibration of functionally graded plates on elastic foundations”, *Compos. Part B*, **159**, 231-247. https://doi.org/10.1016/j.compositesb.2018.09.051.

Zenkour, A.M. (2009), “The refined sinusoidal theory for FGM plates on elastic foundations”, *Int. J. Mech. Sci.*, **51**, 869-880. https://doi.org/10.1016/j.ijmecsci.2009.09.026.

Zenkour, A.M. and Radwan, A.F. (2018), “Compressive study of functionally graded plates resting on Winkler-Pasternak foundations under various boundary conditions using hyperbolic shear deformation theory”, *Arch. Civil Mech. Eng.*, **18**, 645-658. https://doi.org/10.1016/j.acme.2017.10.003.

Zenkour, A.M., Allam, M.N.M. and Radwan, A.F. (2014), “Effects of hygrothermal conditions on cross-ply laminated plates resting on elastic foundations”, *Arch. Civil Mech. Eng.*, **14**, 144-159. https://doi.org/10.1016/j.acme.2013.07.008.

Zine, A., Bousahla, A.A., Bourada, F., Benrahou, K.H., Tounsi, A., Adda Bedia, E.A., ... and Tounsi, A. (2020), “Bending analysis of functionally graded porous plates via a refined shear deformation theory”, *Comput. Concrete*, **26**(1), 63-74. http://dx.doi.org/10.12989/cac.2020.26.1.063.

DC